www.ietdl.org

Published in IET Microwaves, Antennas & Propagation
Received on 3rd November 2013
Revised on 25th March 2014
Accepted on 9th May 2014
doi: 10.1049/iet-map.2013.0605

Special Issue on Emerging Integrated Reconfigurable Antenna Technologies

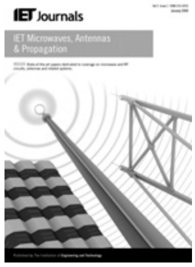

ISSN 1751-8725

Reconfigurable antenna system with a movable ground plane for cognitive radio

Joseph Costantine[1,2], Youssef Tawk[2,3], Jonathan Woodland[4], Noah Flaum[4], Christos G. Christodoulou[2]

[1]*Electrical and Computer Engineering Department, American University of Beirut, Beirut, Lebanon*
[2]*Configurable Space Microsystems Innovations and Applications Center (COSMIAC), University of New Mexico, Albuquerque, NM 87131-0001, USA*
[3]*Electrical and Computer Engineering Department, Notre Dame University, Louaize*
[4]*Electrical Engineering Department, California State University Fullerton, Fullerton, CA 92831, USA*
E-mail: jcostantine@ieee.org

Abstract: A new cognitive radio antenna system is presented and discussed in this study. The antenna system is composed of a wideband antenna that is used for channel sensing and a communicating antenna that is used for dynamic transmission over various frequencies. The communicating antenna is a software controlled reconfigurable antenna that can tune its frequency response by changing the height and angular position of its ground plane. This antenna is composed of a rectangular patch and three ground planes. Two ground planes are fixed while the third one moves and tilts based on the user's demand. The antenna's moving ground plane is controlled by an Arduino board and two linear actuators. The wideband sensing antenna is composed of a printed monopole patch that searches the spectrum for idle frequencies. A prototype of the complete antenna system is fabricated and tested. Both experimental and simulated results show good agreement.

1 Introduction

In recent years, the static spectrum allocation has increased the unbalance in the spectrum usage. Cognitive radio appears to be a solution to this problem by dynamically accessing the spectrum. The dynamic access is completed after channel monitoring and identification of frequencies that are idle, and not used at discrete instants of time. Once these frequencies are identified; the cognitive radio processor, also known as a cognitive engine [1], orders communication over the discovered bands. Thus, a cognitive radio communication scheme is based on two main actions. The first action requires sensing the spectrum and identifying any existing idle frequencies. The second action requires a dynamic capability to communicate over the identified idle frequencies.

The antenna requirements for a cognitive radio system are based on a wideband antenna that senses the channel over a wide bandwidth to identify idle bands. Cognitive radio also requires a reconfigurable antenna that is able to tune its operational frequency to dynamically cover the identified frequencies [1].

There is a need to design a system composed of a reconfigurable antenna and a wideband antenna. For the reconfigurable antenna design, a variety of reconfiguration techniques have been used in the literature. Such techniques include the incorporation of radio frequency-micro electromechanical system (RF-MEMS) [2, 3] or PIN diodes [4–6] as RF switches to connect and disconnect between different antenna parts and elements. Varactors [6, 7] are also used to achieve switching with a variable capacitance values based on the variation in the biasing DC voltage. Although these electrical reconfiguration techniques have been widely implemented and have attracted attention, they have some undesired performance characteristics when they are not designed carefully. Their impedance mismatch with the antenna structure creates a challenge for antenna designers and their reliability consideration needs to be accounted for since their life span can be heavily shortened by problems in harsh environments.

Mechanical reconfiguration techniques, although they achieve slower tuning time for reconfigurable antenna functions, they offer an alternative reconfiguration method with good control over the antenna topology. For example, a pattern reconfigurable square ring patch antenna based on a movable parasitic plate within the ring patch is discussed in [8]. The plate is actuated using a hemispherical dielectric elastomer actuator. Small variations of the height of the parasitic plate can significantly alter the antenna radiation pattern while maintaining reasonable impedance matching. The actuator is used in the antenna by placing it below the parasitic conductor plate. Antenna tuning by varying the antenna's substrate height is also presented in [9, 10] where different instances of substrate heights are discussed for antenna tuning.

In this paper, we present a new cognitive radio antenna system that consists of a wideband printed monopole antenna as well as a new mechanically reconfigurable antenna. The reconfigurable antenna tunes its frequency based on elevating and tilting its ground plane. The radiating patch of the communicating antenna remains stable while the position and angle variation of the ground plane is software controlled.

The paper is divided as follows: in Section 2, we start by presenting the reconfigurable antenna structure, then Section 3 focuses on the reconfigurable antenna's operation. The simulation and measurement results of the proposed reconfigurable antenna structure are shown in Section 4. Section 5 presents the complete cognitive radio antenna system with its sensing antenna component. Section 6 concludes the paper with final analysis of the proposed antenna system.

2 Reconfigurable antenna system structure and design

The proposed reconfigurable antenna is a microstrip line fed patch. The rectangular patch has dimensions of 4.13 cm × 4.85 cm as shown in Fig. 1. The microstrip line feeding the patch has a length of 1.435 cm and a width of 0.12 cm. Two asymmetric rectangular slots are etched on the patch. The first slot (slot 1) has a width of 0.2 cm and a length of 2.4 cm. The second slot (slot 2) is rotated 90° from slot 1 with a width of 0.1 cm and a length of 1.88 cm. The feeding line and the slots dimensions are optimised for a better impedance matching. The slots positions improve the antenna matching and allow a multi-band operation.

The antenna substrate is Rogers Duroid 5880 (RO 5880). It has dimensions of $7 \times 7\ \text{cm}^2$, a height of 0.16 cm and a dielectric constant $\varepsilon_r = 2.2$. The antenna's ground plane is composed of three sections: two fixed ground planes (ground planes 1 and 2) and a moving ground plane as shown in Fig. 2. The two fixed ground planes are positioned as indicated in Fig. 2 and have the dimensions of 7 cm × 0.5 cm for ground plane 1 and 7 cm × 1 cm for ground plane 2. The moving ground plane is rectangular with dimensions of 6 cm × 5 cm. The moving ground plane is controlled by two actuators that allow its vertical movement as well as its tilting position. The actuators used in this work are the Miniature Linear Motion Series L12 by Firgelli Technologies [11] with a positional accuracy up to 0.1 mm. The actuators have a width of 1 cm at the top and a total height of 10 cm. The actuators are powered by four 1.5 V batteries to supply 6 V with a maximum of 400 mA

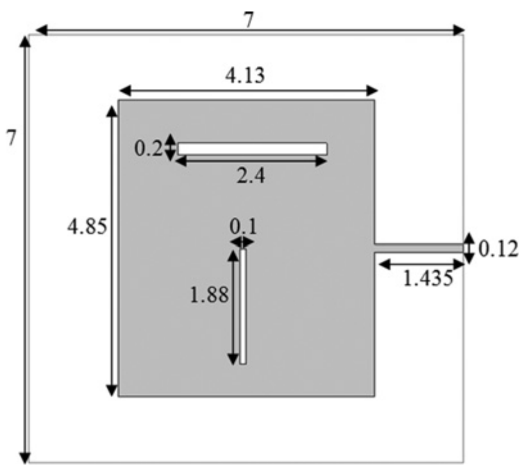

Fig. 1 *Dimensions of the antenna's top layer*

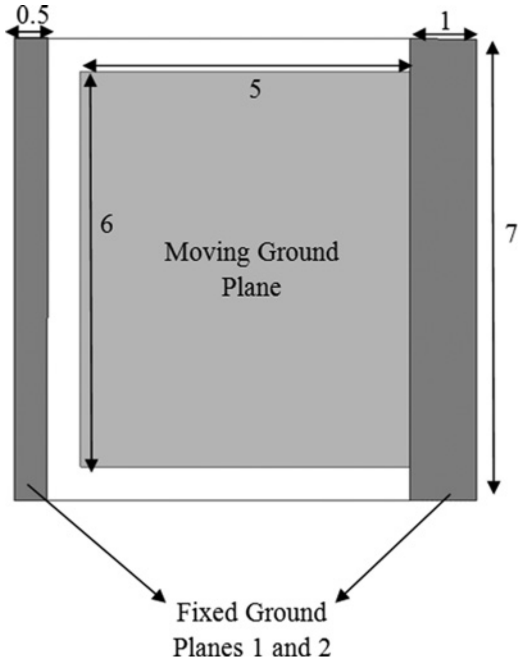

Fig. 2 *Three different parts of the antenna's ground plane*

each. The reconfigurable antenna is designed to cover various frequency bands between 2 and 6 GHz for different ground plane positions and tilt angles.

The fabricated prototype is shown in Fig. 3. The different components of the controlling circuit are enclosed in a foam chassis. An Arduino microcontroller is programmed to receive input from a parallax switch. The output of the Arduino microcontroller feeds the LCD screen as well as the two actuators. The actuators are pulse width modulated with software control by an Arduino board. The software controlling board used in this work is an Arduino Uno R3 [12] with a 5 V voltage supply from a USB port. The antenna system is equipped with a parallax five-position switch [13]. The switch is used to control and drive the ground plane's movement through the Arduino microcontroller. The 'five-position' (PUSH, UP, DOWN, RIGHT and LEFT) parallax switch drives the actuators and thus tunes the antenna's operation. The position of the actuators is indicated on the LCD display [14].

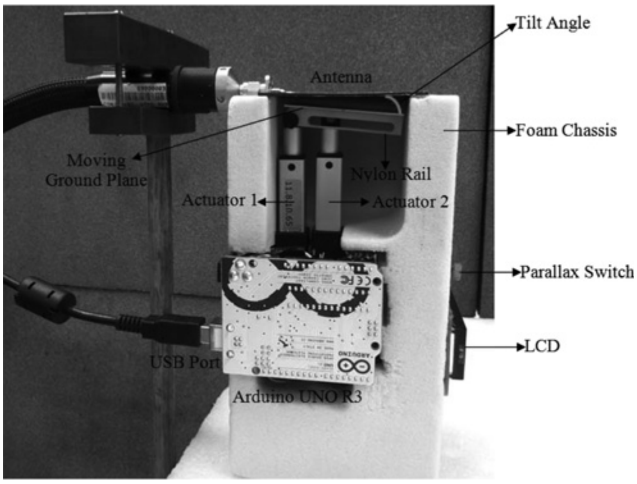

Fig. 3 *Fabricated antenna prototype with the controlling circuit enclosed in foam chassis*

A guide rail links the moving ground to the actuators as shown in Fig. 3. This rail is made of nylon with a dielectric constant of 3.2 and the hooks connecting the actuators to the rail are made of delrin material with a dielectric constant of 3.7. An ultra-dense foam chassis with a dielectric constant of around 1 is chosen to constitute the solid frame that encloses all these different system components. The chassis that encloses the antenna system is of 17 cm height with a 9.5 cm^2 area. The chassis and the rails are included in the simulation.

3 Reconfigurable antenna's operation

The reconfiguration of the antenna's operation is achieved by moving the ground plane vertically or by tilting its position. The vertical movement or tilt introduces an air gap with a variable height. This changes the substrate's effective dielectric constant and transforms the antenna into a suspended microstrip antenna with variable air gap. For the case when the air gap has a zero height, the microstrip antenna behaves as a conventional microstrip antenna [15]. This technique allows the antenna to have a dynamic access to the spectrum and solves the problem of unbalanced spectrum usage. Mechanically tuning the antenna's operating frequencies by changing the position of its ground plane allows the antenna to cover idle bands on demand with a robust user control. It also constitutes an alternative solution to electrical reconfiguration methods that rely on component integration on the antenna's radiating patch.

The strengths of this reconfigurable antenna's design reside in the fact that the radiating patch is fixed and the reconfiguration of the antenna's operation is based on moving a part of the ground plane, thus avoiding the use of any bias lines that can interfere with the antenna's radiation characteristics.

A major antenna capability is based on tuning the antenna's frequency operation over a wide range of bandwidth using software control and with minimum undesired effects. This technique allows the user to control the operational frequencies on demand. A user can change the antenna's frequency of operation by simply changing the ground plane's position. The position of the ground plane controls the operational frequency and allows the antenna to be tuned correspondingly.

3.1 Ground plane's vertical movement

The vertical movement of the ground plane changes the height of the air gap uniformly. As a result, the effective dielectric constant of the combined substrate medium changes since it is dependent on the height of the substrate and the variable air gap. The corresponding structure of the microstrip antenna with the variable dielectric thickness is modelled in Fig. 4 where h_1 is the thickness of the variable air layer and h_2 is the fixed thickness of the antenna substrate. The antenna behaves now as a suspended microstrip antenna with a variable air gap. The modelling of suspended microstrip antennas is discussed in [15, 16]. The resulting dielectric constant of such structure is summarised in (1) [15, 16]

$$\varepsilon_{\text{reff}} = \frac{4\varepsilon_{\text{re}}\varepsilon_{\text{rdyn}}}{\left(\sqrt{\varepsilon_{\text{re}}} + \sqrt{\varepsilon_{\text{rdyn}}}\right)^2} \quad (1)$$

$\varepsilon_{\text{reff}}$ is the effective relative permittivity of the dielectric medium (Rogers Duroid 5880 + variable air gap) [15, 16].

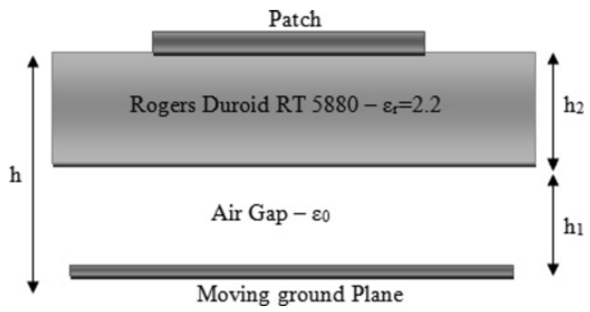

Fig. 4 *Microstrip antenna topology with the ground moving vertically*

ε_{re} is the equivalent permittivity of the two-layer dielectric substrate medium that has a total thickness $h = h_1 + h_2$. ε_{re} is expressed in (2) [16, 17]. $\varepsilon_{\text{rdyn}}$ is the dynamic dielectric constant discussed in [16–18]. It is expressed in (3) as a function of the dynamic main and dynamic fringe capacitances ($C_{0\text{dyn}}$ and C_{edyn}). These dynamic capacitances are also function of the total height of the substrate ($h = h_1 + h_2$) as discussed in [17, 18]

$$\varepsilon_{\text{re}} = \frac{\varepsilon_r\left(1 + (h_1/h_2)\right)}{\left(1 + \varepsilon_r(h_1/h_2)\right)} \quad (2)$$

$$\varepsilon_{\text{rdyn}} = \frac{C_{\text{dyn}}\left(\varepsilon = \varepsilon_0\varepsilon_{\text{re}}\right)}{C_{\text{dyn}}\left(\varepsilon = \varepsilon_0\right)} \quad (3)$$

where

$$C_{\text{dyn}} = C_{0\text{dyn}} + C_{\text{edyn}} = f(h) \quad (4)$$

Equations (1) through (4) show that the effective dielectric constant of the resulting dielectric substrate medium (Rogers Duroid 5880 + air gap) is a function of the height of the total substrate.

Thus varying the air gap thickness, results in varying the effective dielectric constant. This results in tuning of the antenna's operation.

3.2 Ground plane's tilting movement

The antenna topology with a tilted ground plane is shown in Fig. 5. This figure shows the different parameters of the antenna structure at a tilted ground position. W_s/W_p is the width of the substrate/width of the patch; L_s/L_p is the length of the substrate/length of the patch; and H is the height of the tilted ground plane. This height varies from 0 to $(h_1/W_s)W$. In this case, the ground plane is not being dropped uniformly and thus the effective dielectric constant expressed in (1) does not reflect an accurate expression. The volume that is between the ground plane and the substrate can be divided into subsections with variable heights. An integration of the effective dielectric constant expressed in function of W, h and L needs to be completed to obtain an accurate representation of the effective dielectric constant as detailed in (5)

$$\varepsilon_{r\text{Total}} = \int_0^{L_s}\int_0^{W_s}\int_0^{(h_1/w_s)W} \varepsilon_{\text{reff}}\left(w_p, h, L_p\right) dH dW dL \quad (5)$$

doi: 10.1049/iet-map.2013.0605

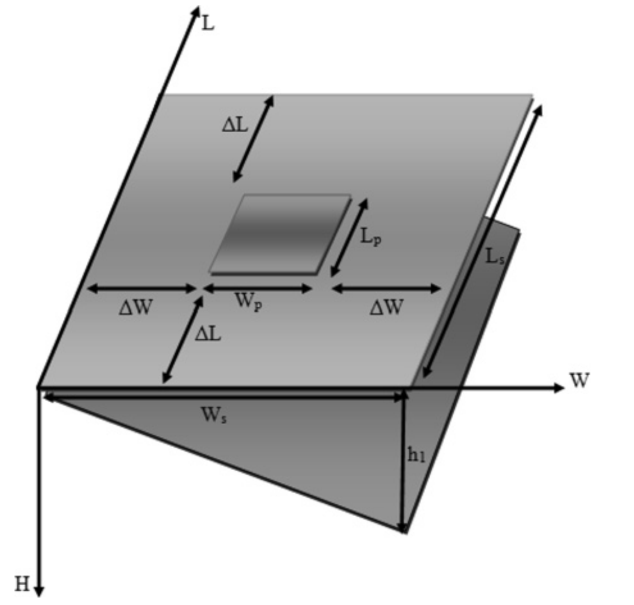

Fig. 5 *Microstrip antenna topology with the tilted ground plane*

where

$$w_p = w_s - 2\Delta w \quad (6)$$

and

$$L_p = L_s - 2\Delta L \quad (7)$$

The effective dielectric constant varies as a function of the air gap thickness in the case where the ground plane is tilted at different angles. Thus changing the tilt angle, changes the thickness h_1 which in turn changes the total effective dielectric constant as shown in (5). This change in the dielectric constant reconfigures the antenna's operation as discussed in Section 4.

4 Reconfigurable antenna results and applications

The antenna system is required to sweep several frequency bands between 2 and 6 GHz and be able to switch between these frequencies dynamically. The designed reconfigurable antenna can tune its frequency of operation to target coverage of applications such as satellite communications, wireless aviation communications, ISM, TV auxiliary broadcasting, private land mobile, earth exploration satellites, radio navigation, WI-FI and WiMAX. The reconfigurable antenna is then proposed for cognitive radio applications because of its ability to widely and dynamically reconfigure its frequency response.

The reflection coefficient of the reconfigurable antenna is measured for different ground plane positions and the results are compared with the simulated data. Good agreement is noticed as shown in Figs. 6*a* and *b* for two different ground plane positions (when the ground plane is dropped by 1 mm and when it is dropped by 3 mm). The frequency reconfiguration is shown in Fig. 7 for five different ground plane elevation positions and tilt angles. The five different ground plane positions correspond to:

– Position 1: $h1 = 0$ mm with a tilt angle of 0°.
– Position 2: $h1 = -1.5$ mm with a tilt angle of 0°.
– Position 3: $h1 = -2$ mm with a tilt angle of 0°.
– Position 4: $h1 = -0.4$ mm with a tilt angle of 0.25°.
– Position 5: $h1 = 0$ mm with a tilt angle of 5°.

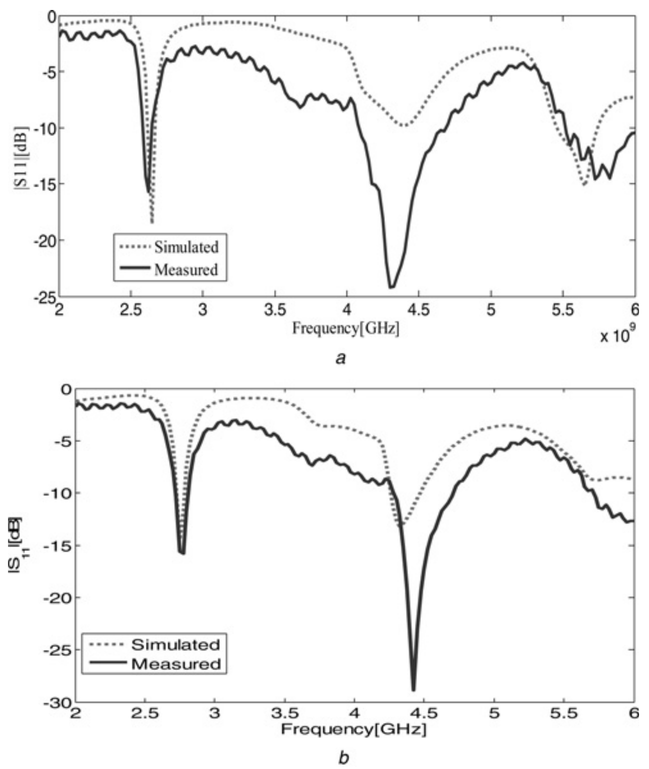

Fig. 6 *Comparison between the measured and simulated reflection coefficient*

a Ground plane is dropped by 1 mm
b Ground plane is dropped by 3 mm

The frequency response shown in Fig. 7 does not exhibit continuous tuning since the changes in the ground plane positions explored in this figure are not continuous. One notices that not all frequency bands have the same bandwidth. This is because of the fact that the reconfiguration is achieved based on either changing the height vertically or titling the ground plane as explained previously. The different positions and orientations of the ground plane affect the antenna's various operational bands

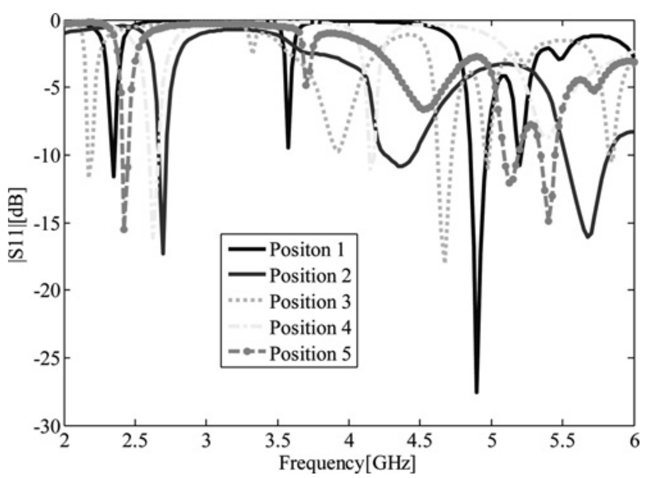

Fig. 7 *Tuning of the antenna frequency response for various ground position and tilt angles*

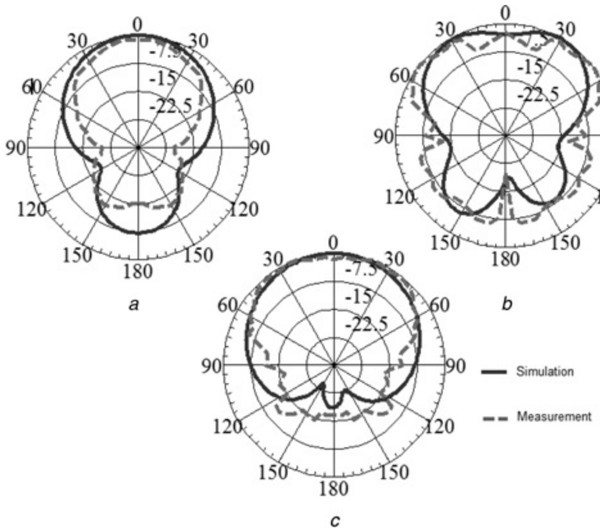

Fig. 8 *Comparison between measured and simulated total radiation pattern (ETotal) in the x–z plane for three different frequencies and ground plane positions*

a f = 2.4 GHz, elevation = 0 mm, tilt angle = 0°
b f = 4.2 GHz, elevation = 0 mm, tilt angle = 5°
c f = 2.75 GHz, elevation = −3 mm, tilt angle = 0°

as well as their bandwidths. The cognitive engine [1] or 'a user' identifies the required frequency of operation and drives the antenna's ground plane using the five-position switch to a predetermined position that will achieve the desired frequency of operation. Thus, operating frequencies are identified, selected and tuned to dynamically cater for the evolving wireless spectrum occupancy. This dynamic control over communicating frequencies allows a much more efficient usage of wireless channels.

The radiation pattern measurements compared with the simulated results are shown in Fig. 8 for three different frequencies of operation as well as three different ground plane positions:

(a) f = 2.4 GHz at $h1$ = 0 mm and tilt = 0°.
(b) f = 4.2 GHz at $h1$ = 0 mm and tilt = 5°.
(c) f = 2.75 GHz at $h1$ = −3 mm and tilt = 0°.

The back lobe shown in the radiation patterns of Fig. 8 is expected and predicted since part of the ground plane is moving and tilting in various directions. A minor back lobe radiation is obtained in Fig. 8*a*. This is expected since at 0 mm, with no tilt, the ground plane is covering most of the antenna's bottom layer. The back lobe is more significant when the ground is tilted as shown in Fig. 8*b*.

5 Complete antenna system for cognitive radio

A cognitive radio system relies on sensing and communicating as its two major functions. The sensing part of the system is achieved by a wideband antenna that monitors the channel constantly between 2 and 6 GHz. The communicating part of the system is the reconfigurable antenna that is discussed in the previous sections. The proposed complete cognitive radio antenna system is shown in Fig. 9.

The sensing antenna is a printed monopole antenna that has a partial ground plane with a size of 4.7 cm × 0.75 cm. It is fed via a stripline that has an opening width of 0.4 cm. The printed monopole antenna with its partial ground achieves a wideband operation between 2 and 6 GHz which makes it beneficial for spectrum sensing in the desired coverage of this antenna system. The trapezoidal feeding section, the patch shape and the partial ground plane are the main reasons for the wideband operation of this antenna. The sensing antenna is positioned out of the plane of the reconfigurable antenna at a height of 4 cm below the surface of the communicating patch. A slit is cut into the hardened foam wall that is supporting the whole antenna system and the sensing antenna is optimally positioned inside the slit. The position of the sensing antenna is optimised for better isolation from the communicating antenna. The isolation between the communicating and sensing antennas remains constant for any position of the ground plane. The reflection coefficient of the sensing antenna is shown in Fig. 10 where good agreement is observed between the simulated and measured results. The radiation pattern for the sensing antenna is

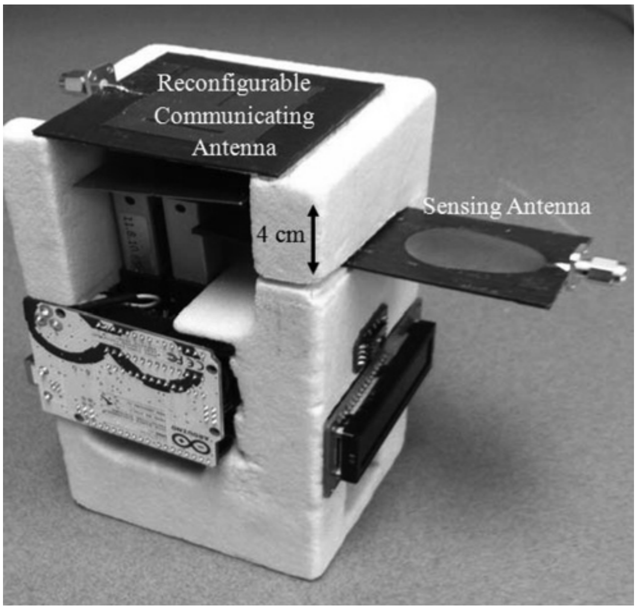

Fig. 9 *Complete antenna system fabricated*

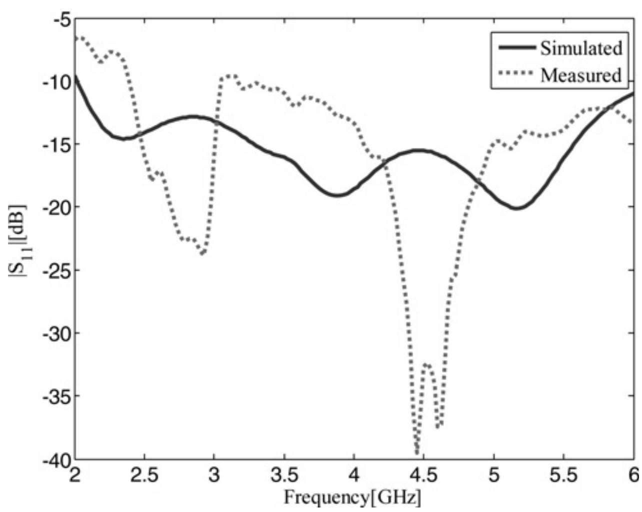

Fig. 10 *Comparison between the measured and simulated reflection coefficient for the sensing antenna*

IET Microw. Antennas Propag., 2014, Vol. 8, Iss. 11, pp. 858–863
doi: 10.1049/iet-map.2013.0605

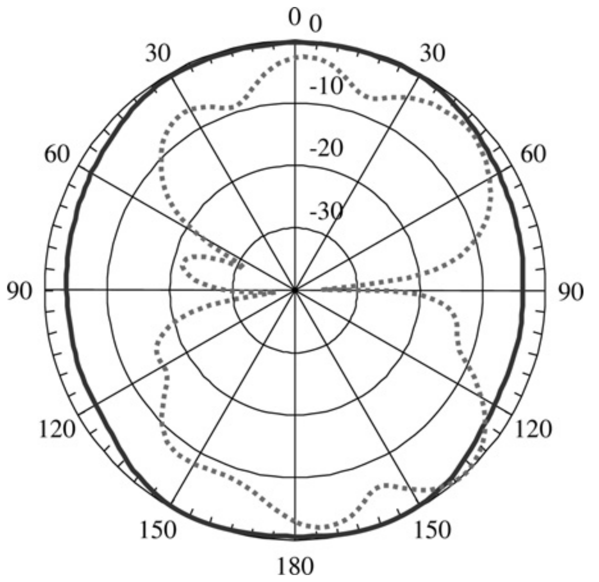

Fig. 11 *Sensing antenna radiation pattern at F = 4.2 GHz*

Dotted line represent the *Y–Z* plane while the solid line represent the *X–Z* plane

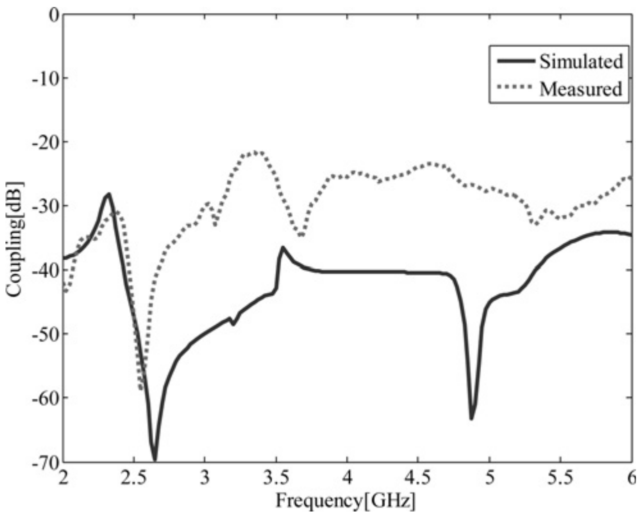

Fig. 12 *Measured and simulated coupling between the sensing and the communicating antenna*

shown in Fig. 11 at $f = 4.2$ GHz for the *X–Z* and *Y–Z* plane cuts. An omni-directional behaviour is noticed in the *X–Z* plane. The coupling between the communicating and sensing antenna is shown in Fig. 12 where good isolation between the two elements is demonstrated.

6 Conclusion

A new mechanically reconfigurable antenna design is presented in this paper as a part of a complete cognitive radio antenna system. The cognitive radio antenna system is composed of two antenna component: a sensing antenna and a reconfigurable antenna with three ground plane sections. Two of the partial ground planes are stationary while the third one (middle section) changes its elevation and tilt angle. The entire system is automated through two actuators that are software controlled through an Arduino microcontroller. A push button drives the system based on orders from the user to change the position of the ground plane and thus tune the antenna's operating frequency. Every step of the process is displayed on an LCD screen enclosed in the package machined out of hardened foam. The sensing and communicating antennas are positioned in such a way to maximise their isolation. The antenna system proposed constitutes a great candidate for software controlled cognitive radio. The system is portable, user friendly and can be controlled on demand by a simple switch configuration. This antenna system adds a new dimension to the reconfigurable software controlled antenna systems that are proposed for wireless communication applications such as cognitive radio. It covers most commercially utilised frequency bands and presents a new reliable venue for mechanically reconfigurable antennas.

7 References

1 Tawk, Y., Bkassiny, M., El-Howayek, G., Jayaweera, S.K., Avery, K., Christodoulou, C.G.: 'Reconfigurable front-end antennas for cognitive radio applications', *IET Microw. Antennas Propag.*, 2011, **5**, (8), pp. 985–992

2 Grau, A., Romeu, J., Lee, M., Blanch, S., Jofre, L., De Flaviis, F.: 'A dual linearly polarized MEMS-reconfigurable antenna for narrowband MIMO communication systems', *IEEE Trans. Antennas Propag.*, 2010, **58**, (1), pp. 4–16

3 Nikolaou, S., Kingsley, N.D., Ponchak, G.E., Papapolymerou, J., Tentzeris, M.M.: 'UWB elliptical monopoles with a reconfigurable band notch using MEMS switches actuated without bias lines', *IEEE Trans. Antennas Propag.*, 2009, **57**, (8), pp. 2242–2251

4 Sarrazin, J., Mahe, Y., Avrillon, S., Toutain, S.: 'Pattern reconfigurable cubic antenna', *IEEE Trans. Antennas Propag.*, 2009, **57**, (2), pp. 310–317

5 Perruisseau-Carrier, J., Pardo-Carrera, P., Miskovsky, P.: 'Modeling, design and characterization of a very wideband slot antenna with reconfigurable band rejection', *IEEE Trans. Antennas Propag.*, 2010, **58**, (7), pp. 2218–2226

6 Jiang, H., Patterson, M., Zhang, C., Subramanyan, G.: 'Frequency tunable microstrip patch antenna using ferroelectric thin film varactor'. IEEE National Aerospace & Electronics Conf., 2009, pp. 248–250

7 Oh, S.S., Jung, Y.-B., Ju, Y.R., Park, H.D.: 'Frequency-tunable open ring microstrip antenna using varactor'. Int. Conf. Electromagnetics in Advanced Applications, September 2010, pp. 624–626

8 Mazlouman, S.J., Soleimani, M., Mahanfar, A., Menon, C., Vaughan, R.G.: 'Pattern reconfigurable square ring patch antenna actuated by hemispherical dielectric elastomer', *Electron. Lett.*, 2011, **47**, (3), pp. 164–165

9 Kitatani, K., Yamamoto, S.: 'Coaxial feed-type microstrip patch antenna with variable antenna height', *Electron. Commun. Jpn. I, Commun.*, 2004, **87**, (2), pp. 10–16

10 Al-Dableh, R., Shafai, C., Shafai, L.: 'Frequency-agile microstrip patch antenna using a reconfigurable MEMS ground plane', *Microw. Opt. Technol. Lett.*, 2004, **43**, (1), pp. 64–67

11 Firgelli Technologies Inc.: 'Miniature Linear Motion Series L12'. Available at http://www.firgelli.com/pdf/L12_datasheet.pdf, accessed 25 June 2013

12 Arduino: 'Arduino Uno'. Available at http://www.arduino.cc/en/Main/arduinoBoardUno, accessed 20 May 2013

13 Parallax Inc.: '5-Position Switch (#27801)'. Available at http://www.parallax.com/Portals/0/Downloads/docs/prod/sens/27801-5PositionSwitch-v1.1.pdf, accessed 3 February 2010

14 Hitachi: 'HD 44780U (LCD II) (Dot Matrix Liquid Crystal Display Controller/Driver)'. Available at http://www.sparkfun.com/datasheets/LCD/HD44780.pdf, 1998

15 Chattopadhyay, S., Biswas, M., Siddiqui, J.Y., Guha, D.: 'Rectangular microstrips with variable air gap and varying aspect ratio: improved formulations and experiments', *Microw. Opt. Technol. Lett.*, 2009, **51**, (1), pp. 169–173

16 Guha, D., Antar, Y.M.M.: 'Microstrip and printed antennas: new trends, techniques and applications' (John Wiley and Sons, 2011)

17 Wolff, I., Norbert, K.: 'Rectangular and circular microstrip disk capacitors and resonators', *IEEE Trans. Microw. Theory Tech.*, 1974, **22**, (10), pp. 857–864

18 Guha, D.: 'Resonant frequency of circular microstrip antennas with and without air gaps', *IEEE Trans. Antennas Propag.*, 2001, **49**, (1), pp. 55–59